Lasers Med Sci (2015) 30:2369–2379
DOI 10.1007/s10103-015-1823-5

ORIGINAL ARTICLE

Atomic force microscopy investigation of the interaction of low-level laser irradiation of collagen thin films in correlation with fibroblast response

Andreas Stylianou[1] · **Dido Yova**[1]

Received: 31 May 2014 / Accepted: 16 October 2015 / Published online: 24 October 2015

Abstract Low-level red laser (LLRL)–tissue interactions have a wide range of medical applications and are garnering increased attention. Although the positive effects of low-level laser therapy (LLLT) have frequently been reported and enhanced collagen accumulation has been identified as one of the most important mechanisms involved, little is known about LLRL–collagen interactions. In this study, we aimed to investigate the influence of LLRL irradiation on collagen, in correlation with fibroblast response. Atomic force microscopy (AFM) and fluorescence spectroscopy were used to characterize surfaces and identify conformational changes in collagen before and after LLRL irradiation. Irradiated and non-irradiated collagen thin films were used as culturing substrates to investigate fibroblast response with fluorescence microscopy. The results demonstrated that LLRL induced small alterations in fluorescence emission and had a negligible effect on the topography of collagen thin films. However, fibroblasts cultured on LLRL-irradiated collagen thin films responded to LRLL. The results of this study show for the first time the effect of LLRL irradiation on pure collagen. Although irradiation did not affect the nanotopography of collagen, it influenced cell behavior. The role of collagen appears to be crucial in the LLLT mechanism, and our results demonstrated that LLRL directly affects collagen and indirectly affects cell behavior.

✉ Andreas Stylianou
styliand@mail.ntua.gr; andreas.c.stylianou@gmail.com

[1] Biomedical Optics and Applied Biophysics Laboratory, School of Electrical and Computer Engineering, National Technical University of Athens, Iroon Polytechniou 9, 15 780 Athens, Greece

Keywords Atomic force microscopy (AFM) · Collagen · Fibroblasts · In vitro · Low-level laser therapy (LLLT) · Low-level red laser (LLRL)

Introduction

Low-level laser irradiation (typically 500–1100 nm) of cells has recently been found to have a wide range of medical applications, and its effects on tissue or individual tissue components are of increasing interest [1–4]. In recent decades, low-level laser therapy (LLLT) has become increasingly popular for treating a wide range of medical conditions because irradiation at these energy densities (typically involving delivery of 1–4 J/cm^2 to the treatment site [1, 2]) accentuates cellular biochemical reactions. The resulting reactions reduce tissue edema and inflammation, phagocytosis, collagen deposition, protein synthesis, and epithelialization and improve the tensile strength of tissues [5, 6]. Among the more promising applications are the biostimulation of wound healing [7] and the improvement of the healing process in a variety of pathological conditions, such as burns [8]. The mechanism associated with photobiostimulation by LLLT is not yet fully understood, although it appears to be due to the modulation of certain cellular types that comprise the healing microenvironment [9]. Although LLLT is now used to treat a wide variety of ailments, it remains somewhat controversial, because uncertainties remain concerning its fundamental molecular and cellular mechanisms, and a large number of dosimetry parameters must be controlled [5].

Studying the effects of LLLT on extracellular matrix (ECM) elements, such as collagen, is important to understand how it affects the wound healing process. Because the healing process is complex and involves a series of events (including clotting, inflammation, granulation tissue formation,

epithelialization, collagen synthesis, and tissue remodeling), it must be researched extensively to identify factors that could delay or hinder the process [8]. Although a large number of reports demonstrating the positive effects of LLLT in various in vitro, in vivo, and clinical studies have been published [10–12], little is known about the effect of laser light on collagen.

Collagen type I is the most prevalent ECM protein and is located in skin, bone, tendons, and cartilage [13]. The molecular unit of type I collagen (length ~300 nm, diameter ~1.5 nm) is fibrous and is composed of three polypeptide chains wrapped together into a semi-flexible triple helix [14]; the triple helixes are assembled to form fibrils which are aligned laterally into bundles and fibers. Collagen fibrils are the elementary building blocks of collagen-rich tissues and support other bodily tissues. Furthermore, collagen is important for a variety of functions, including tissue scaffolding, angiogenesis, and tissue repair [15]. Additionally, collagen contains amino acid sequences that may be recognized by specific receptors, and cells have been shown to respond to the mechanics, topography, and structure of the collagen matrix [16, 17]. Through its influence on the interactions between cells and ECM, it controls growth, differentiation, metabolism, and gene expression. Therefore, modifying the surface properties of collagen can improve or destroy cell alignment, adhesion, and proliferation [18].

LLLT has been shown to contribute to increased expression of collagen and elastic fibers during the early phases of the wound healing process [9]. Moreover, laser irradiation has been demonstrated to improve the arrangement of collagen fibers, which is necessary for development of the tensile force of the cicatricial tissue. The increased number of collagen fibrils and fibers in the ECM following laser treatment may result from a combination of fibroblast proliferation and enhanced collagen synthesis by these cells [19]. Laser treatment may act by stimulating either one or both simultaneously. Similar data have been presented in relation to bone and ligament repair [20, 21]. Although all of these studies have indicated that LLLT plays a decisive role in determining the amount and quality of the collagen produced by fibroblasts during wound healing, the influence that low-level laser irradiation may have on collagen itself has not been clarified.

In this study, we aimed to investigate the influence of low-level red laser (LLRL) on collagen by developing a well-characterized collagen-based surface with controlled topography of collagen thin films in the nanoscale range. We quantified the surface modification of collagen induced by LLRL and examined correlations with cell alterations. Our investigation focused on short exposure times to LRLL and doses relevant to LLLT. Thin collagen films were used because they can act as substrates for culturing cells, and their surface can be characterized with atomic force microscopy (AFM), which is a powerful quantitative and qualitative tool [22, 23]. AFM can be used for investigating tissue alterations, such as the natural healing process and the regeneration of collagen after laser treatment [24], and shows excellent performance for investigating films similar to the ones used in this study [18, 25, 26].

Materials and methods

Collagen stock solution

Type I collagen from bovine Achilles tendon (Fluka 27662, Sigma-Aldrich) was dissolved in acetic acid (CH_3COOH 0.5 M) to a final concentration of 8 mg/mL and stored at 4 °C for 24 h. The solution was then homogenized at 24, 000 rpm (Homogenizer IKA T18 Basic, Staufen, Germany) and stored at 4 °C as the stock solution. Part of the stock solution was diluted with phosphate-buffered saline (PBS) to a final concentration of 1 mg/mL. Part of the stock or the 1 mg/mL solution was laser irradiated, and both irradiated and non-irradiated collagen solutions were used for collagen thin film formation.

Collagen thin film formation

Collagen thin films were formed by spin coating (SpC) (Spin Coater WS-400B-6NPP/LITE, Laurell Technologies) using both irradiated and non-irradiated collagen solutions. Collagen solution (50 μL) was flushed onto fresh-cleaved mica discs (71856–01, Electron Microscopy Science, Hatfield, PA) and SpC for 40 s at 6000 rpm.

LLRL irradiation of collagen

The collagen solution was irradiated in air using a 661-nm diode laser system (GCSLS-10-1500 m, China Daheng Group, Inc., Beijing, China), accompanied with an optical fiber with diffuser. The experiments were performed in 1-cm cuvettes, and the solution was constantly stirred with a micro-submersible magnetic stirrer (Model MS-7, TRI-R Instrument, Inc., Rockville Center, NY) placed inside the cuvette. The collagen solutions and films were placed 4 cm from the light. The fluence rates were measured with a power meter with a laser thermal low power sensor (Nova display with a 3A-FS-SH puck, Ophir Laser Measurement Group, North Logan, USA) and adjusted to 4 mW/cm^2.

Collagen samples (solutions or films) were irradiated after formation, and the irradiation was repeated several times to simulate LLLT, in which tissue is treated with laser at specific time intervals [5, 8, 27]. Sufficient time was allowed between treatments to avoid laser-induced thermal effects. Table 1 shows the irradiation parameters. All measurements were performed at the same

Table 1 Irradiation parameters

Laser		GCSLS-10-1500 M	
Frequency		Continuous	
Power		7 mW	
Power density		8.9 mW/cm^2	
Spot size		0.785 cm^2	
Energy density		4 J/cm^2	
Time per point		45 s	
Treatments	0	No treatment	
	a	5×45=225 s	5×4 J/cm^2
	b	10×45=450 s	10×4 J/cm^2
	c	15×45=675 s	15×4 J/cm^2
	d	20×45=900 s	20×4 J/cm^2

temperature to avoid any influence on the physicochemical properties of collagen.

Fluorescence studies

Emission spectra of the collagen solution and films were recorded before and after laser irradiation using a fluorescence spectrophotometer (PerkinElmer LS 45, Luminescence Spectrometer, MA, USA). The samples were excited at 253 nm, which is the maximum excitation wavelength of phenylalanine residues [28], and the fluorescence emission maximum was monitored.

AFM imaging

AFM images of the collagen films were obtained in air using a commercial microscope (CP II, Vecco Bruker Metrology, Santa Barbara, CA). All images were obtained at room temperature in tapping mode using typical anisotropic AFM probes (MPP-1123, Bruker). The samples were mounted on AFM metal discs with epoxy glue, and locator grids (copper finder grid, G2761C, Agar Scientific, Essex, UK) were used to map the surface. Images of various sizes were captured of each sample at several locations; only representative illustrations are shown. Surface images, with a scan rate between 0.5–1 Hz, were acquired at a fixed resolution (512×512 data points).

Cell culture

A human dermal primary fibroblast cell line was used in all experiments (passages 4–12). The cells were cultivated in 25-cm^2 culture flasks (Corning, New York, USA) in Complete Cell Culture Medium (CCCM) containing Dulbecco's modified Eagle's medium (DMEM, Gibco, Life Technologies, Paisley, UK) supplemented with 10 % heat-inactivated fetal bovine serum (FBS) (Gibco), and 0.1 % antibiotic–antimitotic (Gibco). Cells were stored at 37 °C in a 5 % CO_2 humidified incubator, trypsinized, and re-seeded into fresh medium every 6–7 days.

Seeding cells on films

Prior to seeding of cells on the samples, the substrates were rinsed twice with PBS containing 0.1 % antibiotic–antimitotic and were conditioned for 30 min with the CCCM described above. During this period, the films were stored at 37 °C in the humidified incubator. Cells were removed from tissue culture flasks by trypsinization and plated at a density of 2×10^5 cells/dish in a petri dish containing a substrate in CCCM. Care was taken to ensure the seeding density was homogeneous over the substrates. Cells were grown in CCCM for 3 days before being imaged with fluorescence microscopy.

Fluorescence microscopy imaging of cells

Cells were imaged with fluorescence microscopy using rhodamine B, which can be used as a probe for assessing cells' mitochondrial matrix [18]. The films with the seeded cells were incubated for 10 min at 37 °C in a 5 % CO_2 humidified incubator in CCCM containing 1.2 μM rhodamine B. Fluorescence microscopy studies were performed using an epifluorescent microscope (Olympus BX-50, Olympus Optical Co. GmbH, Tokyo, Japan). Regions of interest were imaged using both phase contrast and fluorescence imaging modes. Images were acquired with an Olympus 20×, UPlanFl, 0.50 NA. The fluorescence microscope was equipped with a 100-W mercury arc light for excitation using appropriate optical filter sets for each dye. The filter cubes for rhodamine B were configured as follows: excitation BP510-550, dichroic mirror DM570, and emission BA590. Images were acquired with a charge-coupled device (CCD) color camera (Olympus XC30). For in vivo microscopic observation of cells, a small perfusion chamber was used, as described previously [29]. The thin films with the seeded cells were mounted upside down in the perfusion chamber, which was filled with 4-(2-hydroxyethyl)-1-piperazineethanesulonic acid (HEPES)-Hanks balanced buffer, via the hydrostatic perfusion system.

Image processing

AFM image processing and quantitative measurements were performed using the image analysis software that accompanied the AFM system, DI SPMLab NT ver.60.2 (Veeco) and the freeware scanning probe microscopy software WSxM 5.0 dev.2.1 [30].

Additionally, image analysis of fluorescence microscopy images was performed using ImageJ (NIH, Bethesda)

software. ImageJ was used to assess cell elongation and area. The *elongation* (*E*) factor of cells was calculated using the formula $E = \frac{Long\ \ Axis}{Short\ \ Axis} - 1$ [18]. The *E* factor describes the extent to which the equimomental ellipse is lengthened or stretched out. Thus, *E* is 0 for a circle and 1 for an ellipse with an axis ratio of 1 : 2. Thus, the cells that presented *E* values 0–0.5 were considered as spherical, 0.5–1 as ellipsoid, and *E* values higher than 1 as elongate [18]. For the measurement of the long and short axes, the filopodia of the fibroblasts were excluded. The elongation of the nucleus was also assessed. For quantitative investigation of cell characteristics, approximately 100 cells, for at least three different samples from each different condition, were measured.

Statistical analysis

The values of the measurements were expressed as the mean ±standard deviation. Fluorescence intensity measurements were analyzed with OriginPro 8 SR0 (OriginLab Corporation), and linear and polynomial fitting were performed by using OriginPro's routines. Experimental groups were compared using an unpaired Student's *t* test. Statistical significant difference was determined when $p<0.05$.

Results

Fluorescence spectroscopy of LLRL-irradiated collagen

Fluorescence spectroscopy was used to determine if collagen was photostimulated by the LLRL wavelengths and doses used. Figure 1a shows the fluorescence spectra of the original collagen solution (1 mg/mL). Excitation at 253 nm generated two emission peaks (at 345 and 420 nm) for the native collagen solution. These peaks are in concordance with previous literature, in which it was demonstrated that acidic collagen solutions show the fluorescence spectrum presented here and that the peaks are influenced by the concentration and aggregation of the collagen [31].

After laser irradiation for various time intervals (treatments), the fluorescence spectra of the collagen solution maintained their characteristic maxima, but the emission intensity was altered. Figure 1b shows the fluorescence maxima measured after irradiation of the collagen solution (squares) and thin films formed by the laser-irradiated collagen solution (circles). Increasing the duration of irradiation produced a small gradual increase in the fluorescence emission in both samples (for the solution, the initial fluorescence was 371.03±2.73 a.u. and the final was 413.85±0.39 a.u., while for the film it was 204.84±0.58 and 216.21±0.55 a.u., respectively). Furthermore, the linear fitting of the values demonstrated that solution and film samples presented positive values of the slope, 2.98±0.33

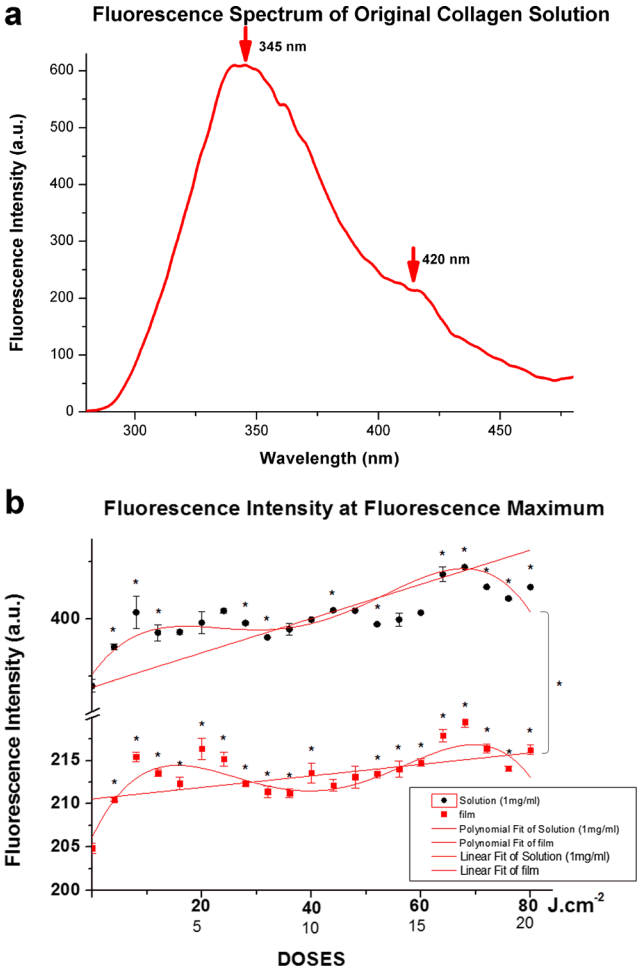

Fig. 1 Fluorescence spectrum of the original collagen solution (**a**) and fluorescence intensity of collagen solution at fluorescence maximum after laser irradiation (**b**). For Fig. 1b, each measurement was compared for statistical significance with the initial measurement without irradiation dose (*asterisk* indicates statistical significance of $p<0.05$). Also, all the measurements for irradiation of the collagen solution were compared with the measurements for irradiation of the film (the *bracket* and the *asterisk* on the right of the figure indicate that all the measurements presented statistical significance of $p<0.05$)

and 0.27±0.06, respectively (see Fig.1b linear fitting).The difference in fluorescence intensity between the solution and the film is due to the different types of samples and to the fact that the solutions were measured in a 1-cm cuvette, whereas the films were formed by SpC and were extremely thin. Complex fluorescent molecules, such as collagen, have more than one fluorophore, and changes in the structure of these molecules also alter their fluorescence spectrum [32].

AFM imaging of LLRL-irradiated collagen films

The use of the SpC enabled the formation of thin films consisting of randomly oriented fibrils/fibers [18, 25, 26] (Fig. 2, 0). A transverse D-banding periodic pattern consisting of grooves and ridges could be clearly observed in the fibril

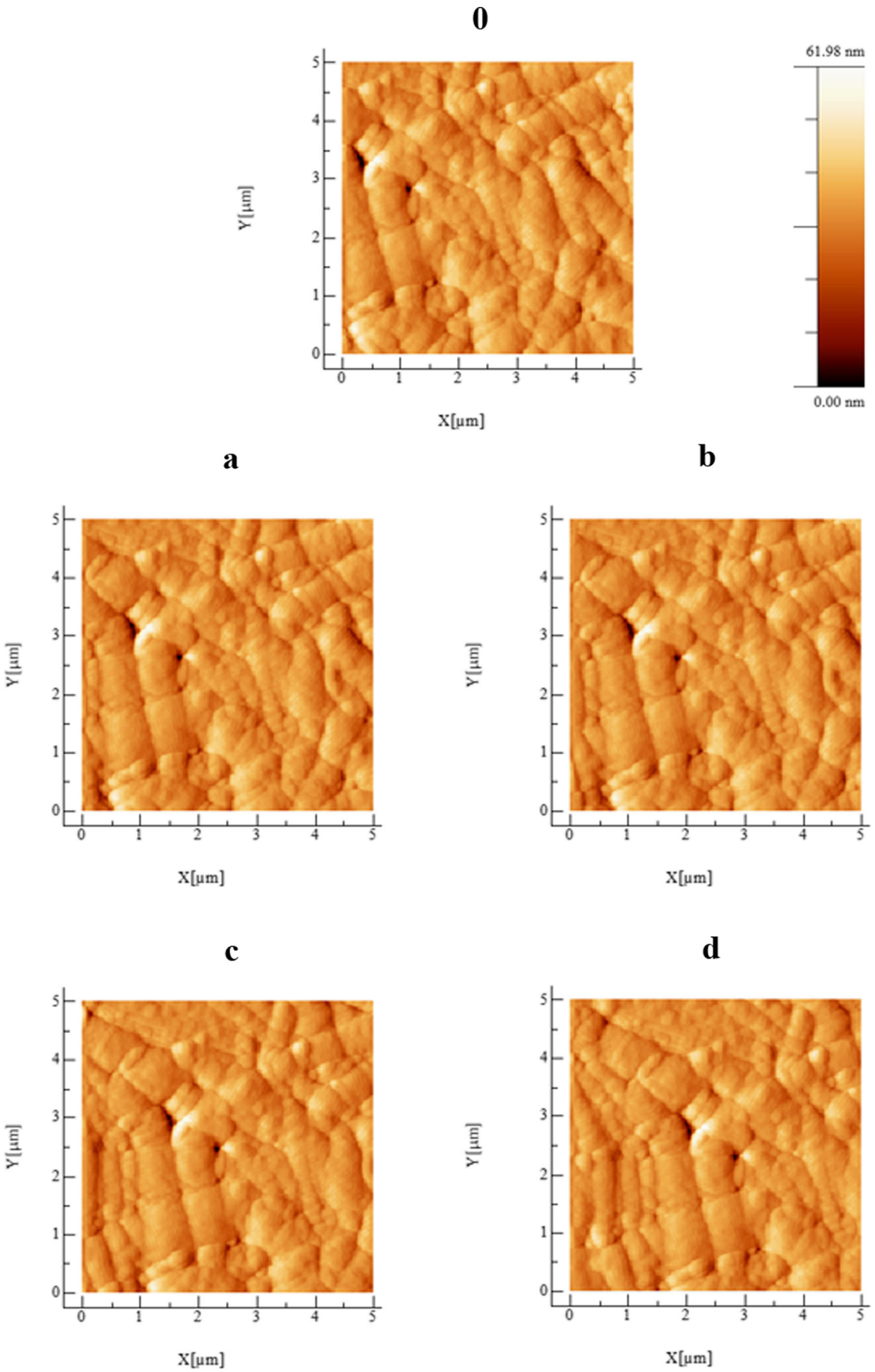
0
61.98 nm
0.00 nm
Y[µm]
X[µm]
a
b
c
d

◀ **Fig. 2** Atomic force microscopy (AFM) topographic images (5×5 μm) of collagen films irradiated with different doses (**0** no dose, **a** 1×4 J/cm^2, **b** 2×4 J/cm^2, **c** 3×4 J/cm^2, and **d** 4×4 J/cm^2)

images. The average distance between the neighboring grooves was approximately 67 nm, similar to naturally occurring fibrils [13]. The collagen films formed with this nanostructure because collagen molecules naturally self-assemble; in vivo self-assembly is entropy-driven and is responsible for the characteristic D-banding pattern [13]. In vitro, collagen self-assembly occurs via both linear and lateral growth steps, with parallel events to those observed in vivo; however, in the absence of cellular control and enzymatic cleavage of propeptides, the growth mechanism is altered [33]. The remaining images (a–d) in Fig. 2 show the same area after the film was irradiated with different doses of LLRL. Irradiation did not induce any significant alterations of the surface topography of the thin films. Fiber diameter, orientation, and average height remained constant. Surface roughness measurements also demonstrated that roughness was not altered by irradiation.

Because the D-periodicity of collagen is crucial [13, 14, 16], the influence of laser irradiation on the D-banding of collagen fibrils was investigated. An area of a collagen thin film (where the D-band of several collagen fibrils could clearly be observed) was selected for monitoring D-periodicity alterations after LLRL irradiation (Fig. 3). As Fig. 3 shows, the LRLL doses used in this study did not alter the D-banding, and height profile measurements confirmed that the groove-to-ridge distances did not change measurably.

Culturing cells on LLRL-irradiated collagen films

The SpC collagen films were used as substrates for culturing primary human skin fibroblasts. Fibroblast morphology and alignment were assessed with fluorescence imaging and image analysis techniques. Fluorescence images of the adherent cells on the thin films are shown in Fig. 4. Qualitatively, the fluorescence images show that untreated fibroblasts had a more elongated structure, which is considered their native form (Fig. 4, 0). The fibroblasts were fusiform or spindle-shaped, usually with two filopodia extending in opposite directions. However, as the LLRL dose increased, fibroblasts became ellipsoidal or even spherical (Fig. 4a–d). Moreover, the number of filopodia per fibroblast increased as the dose increased.

To obtain quantitative data on cell shape, the elongation of fibroblasts and nuclei was assessed using image analysis. Figure 5a, b shows the elongation of the cell body and the nucleus, respectively. From the charts, it can be seen that for each separated dose, the values of the cell body elongation/nucleus elongation in the three groups (spherical, ellipsoid, and elongate) are similar. Statistical analysis demonstrated that there is no significant difference between the elongation values of each group for the different doses comparing with the initial value of elongation for 0 dose (data are not presenting). On the other hand, for each dose, the differences between each group were statistically significant. Although, for each dose, the values of elongation were not different, the percentage of the cells that belonged to each category was modified. Charts showing the percentage of cell and nucleus elongation are presented in Fig. 5c, d, respectively. Prior to irradiation, the majority of the fibroblasts were the elongated type (59.0± 1 %), and only a small percentage of the fibroblasts were spherical (19.0±5.0 %; Fig. 5c). As irradiation of the collagen thin film increased, the percentage of elongated fibroblasts decreased. Simultaneously, the number of spherical cells increased. For the final dose, the 32.9+0.2 % belonged to the elongated type and 42.9±5.7 % belonged to the spherical type. A similar pattern was observed in fibroblast nuclei, although the majority of the nuclei had a more ellipsoidal shape following irradiation (Fig. 5d). Prior to the irradiation, the 59.0±4 % were elongated and 26.0±4.0 % were spherical, and for the final irradiation, the parentage was modified to 24.3±1.4 and 35.7±4.2 %, respectively.

Discussion

In this study, we aimed to investigate the influence of LLRL on collagen directly, in correlation with fibroblast response. The majority of studies published to date have focused on fibroblast behavior, stimulation of collagen production, and improvement of the healing process in damaged tissue. In contrast, this investigation sought to characterize LLRL-induced alteration of collagen and to identify possible modifications in fibroblast behavior. The doses applied were similar to those used previously for stimulating the healing process [5, 8, 9], because the appropriate energy density for wound healing has been reported to be 1–4 J/cm^2 [34]. Previous studies have demonstrated that the wavelength used here is appropriate for LLLT [8, 27].

Studies published to date on the LLLT–collagen relationship have emphasized the importance of the increased production of new collagen reported during LLLT and have attempted to investigate the various parameters involved. The enhancement of collagen accumulation has been reported to depend on the wavelength used [5], and in many cases, the new collagen has been reported to consist of more dense and aligned collagen fibers [27]. Increased proliferation of fibroblastic cells and/or increased anabolic cellular activity has been identified as potential mechanisms for the increased deposition of collagen during LLLT [9].

The results of this study demonstrated that LLRL induced rather small alterations in the fluorescence emission of collagen; a negligible influence on collagen thin film topography

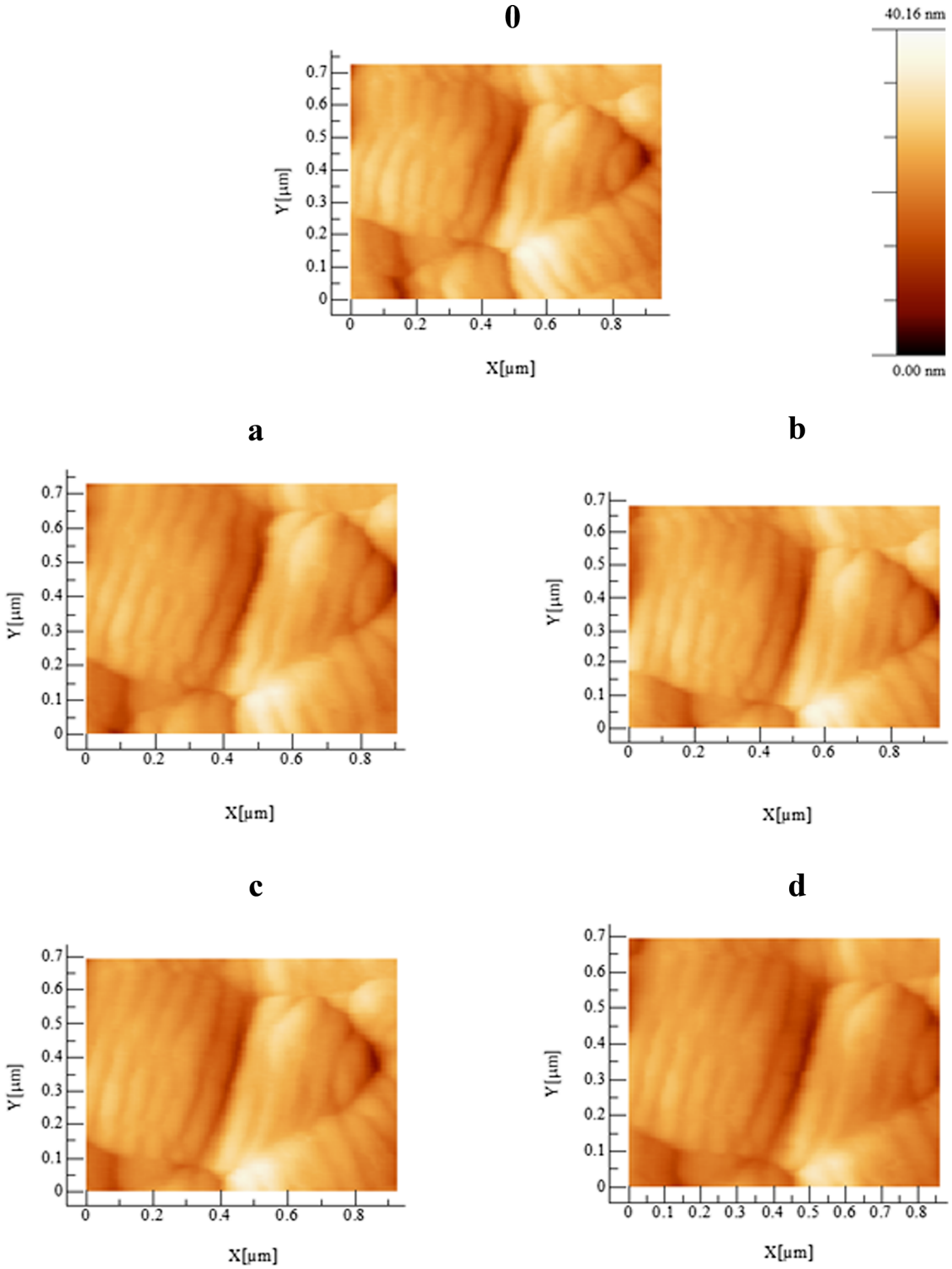

Fig. 3 AFM topography images of D-banding of collagen films irradiated with different doses (**0** no dose, **a** 1×4 J/cm^2, **b** 2×4 J/cm^2, **c** 3×4 J/cm^2, and **d** 4×4 J/cm^2)

was observed after irradiation. The small alteration in the fluorescence emitted from collagen shown here may be a sign of changes in collagen conformation or cross-linking. Collagen-linked fluorescence has been reported to increase with age in many organs and tissues in vivo [35, 36]. This increase is attributed to increased amounts of advanced glycation end products (AGEs), which are responsible for protein cross-linking [37, 38]. Moreover, an increase in fluorescence caused

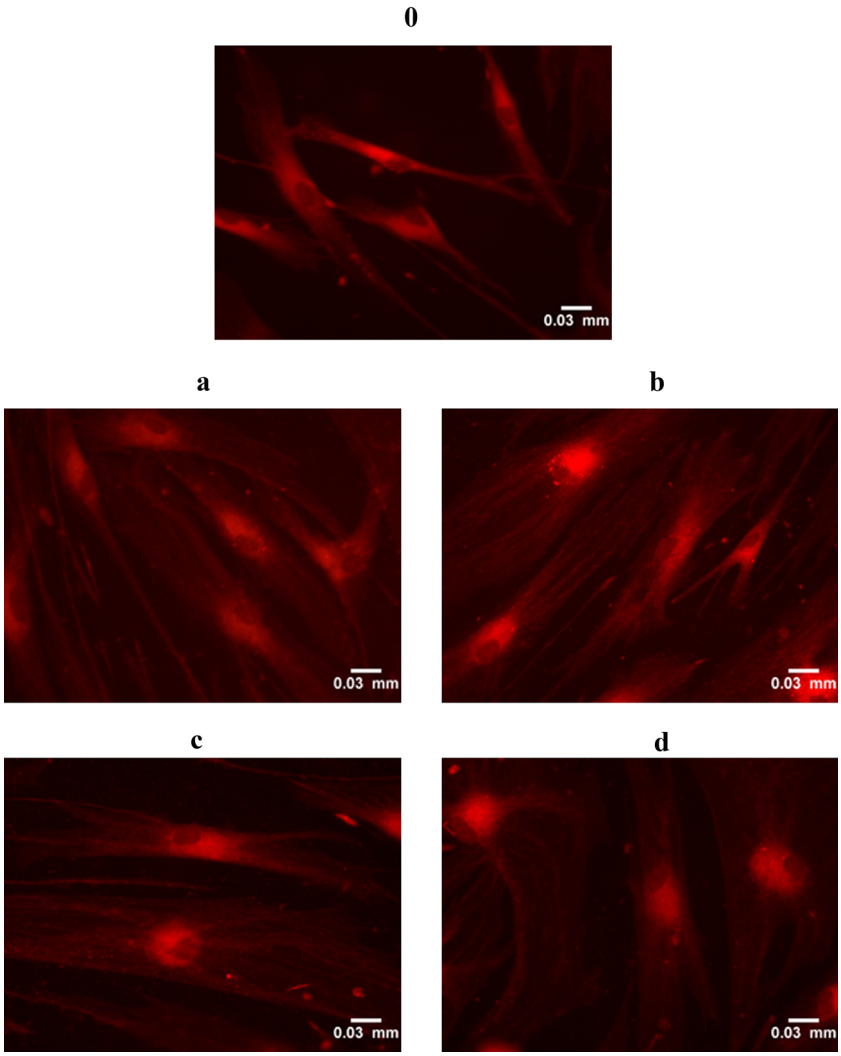

Fig. 4 Fluorescence images of fibroblast cultures on irradiated thin films. Irradiation was administered at varying doses (**0** no dose, **a** 1×4 J/cm^2, **b** 2×4 J/cm^2, **c** 3×4 J/cm^2, and **d** 4×4 J/cm^2)

by enhancement of AGE production has been reported in diabetic patients [37, 39]. These possible changes may differentiate the mechanism of collagen–cell interactions and explain a portion of the observed differences in cell behavior.

Film topography, including surface roughness and nanoscale characteristics of the collagen fibers (D-band periodicity, groove-to-ridge distances, and fiber diameter), did not display post-irradiation changes. However, fibroblasts cultured on LLRL-irradiated collagen thin films responded to irradiation. As the dose increased, both cells and nuclei became increasingly spherical. In this particular cell line (primary human fibroblasts), this is an indication of abnormal growth. These changes in cell behavior occurred in the absence of measurable changes in collagen topography. Similar fibroblast behavior has been reported on ultraviolet (UV)-irradiated collagen thin films [40]. Differentiation of fibroblast behavior under the influence of UV irradiation was correlated with alterations of collagen surface properties such as topography, surface roughness, and mechanical properties, and collagen photodegradation was a possible effect parameter. However, the LLRL irradiation employed in this study caused changes in cell behavior in the absence of measurable changes in collagen topography. Therefore, surface-based cell guiding mechanisms, such as the "contact guidance mechanism" [41], could not have influenced fibroblast behavior. Consequently, the fibroblast response could be correlated with other types of collagen differentiation induced by laser light. Further research should focus on possible alterations of the mechanical properties of collagen and on collagen-to-cell signaling mechanisms prior to and post-laser irradiation.

The mechanical properties of the ECM can alter cell morphology, mobility, differentiation, and proliferation rate [17, 42], and stiffer matrices promote cell spreading and proliferation [43]. Although several potential mechanisms have been proposed for collagen-to-cell interactions, the process is complex and the complete mechanism has not yet been fully clarified [44]. Generally, inhibition or modulation of the normal cell growth cycle by the extracellular matrix may be derived from the biochemical and/or physical properties of cell contact with the ECM [44, 45]. Apart from mechanical properties,

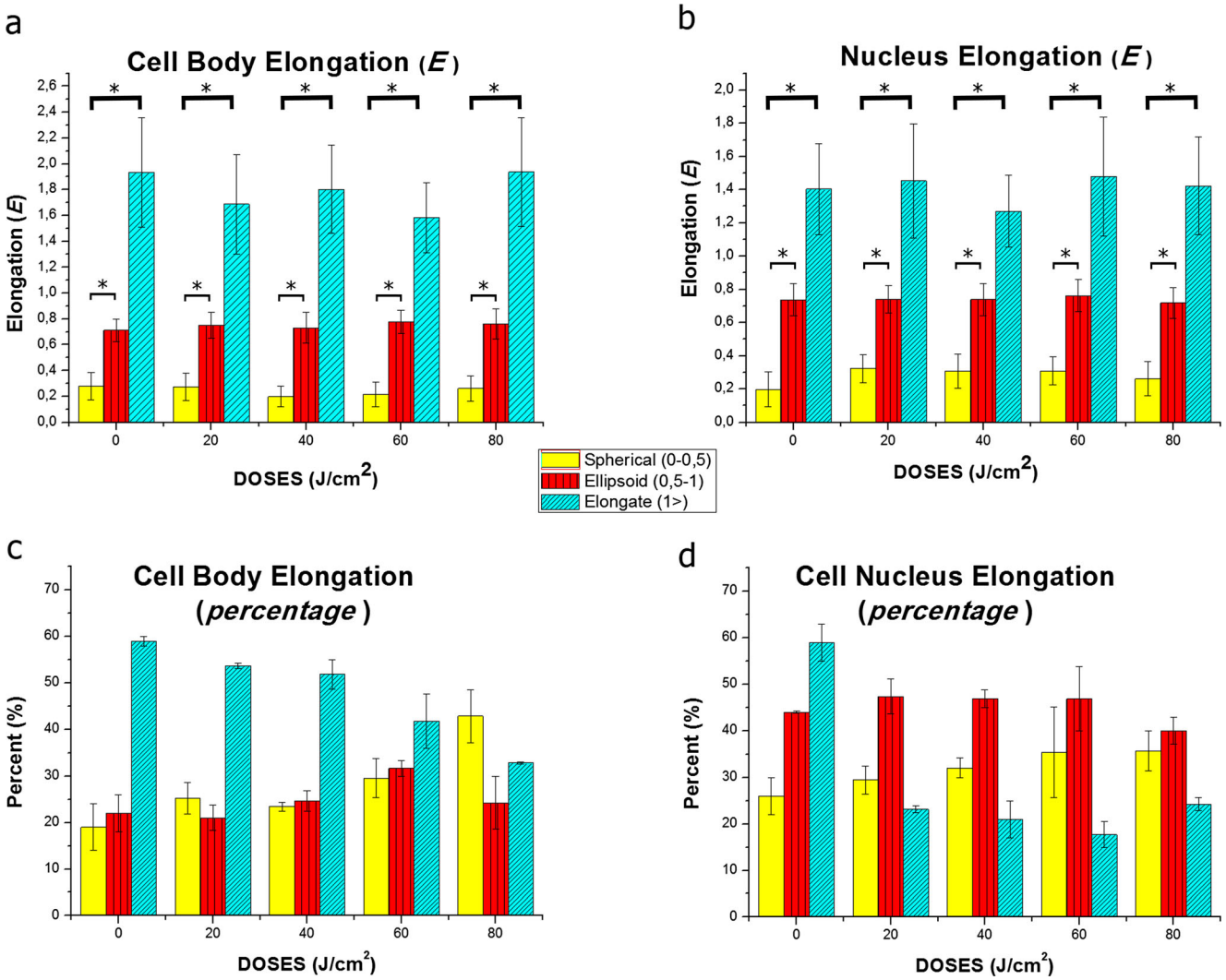

Fig. 5 Charts presenting the elongation of cells (**a**) and nuclei (**b**) on the different irradiated substrates. Charts **c** and **d** show the percentage of cell and nucleus that belong to each elongation group for each dose

changes in cell behavior may be caused by changes in the conformational structure of collagen, which affects the binding of cells to collagen via appropriate receptors. Several integrins, as well as non-integrin receptors, bind to distinct regions of type I collagen, depending on whether the collagen is in its native or denatured conformation [14]. Therefore, the small alteration in the fluorescence emission observed after LLRL irradiation may indicate the initiation of differentiation of collagen conformation or growth linkages. These changes may differentiate the mechanism of interaction and/or collagen–cell signaling and partially explain the observed differences in cell behavior.

In previous LLLT studies, abnormal cell growth was not reported, perhaps because irradiation was performed mainly in the tissues and the cells themselves. Moreover, the collagen fibrils/fibers in tissues are usually covered by other proteins and proteoglycans, and consequently, collagen structures are protected from irradiation and are inaccessible by cell receptors [14]. Furthermore, irradiation of cells themselves with the doses used in LLLT has been shown to enhance cellular function, and it is therefore likely to overcome the possible negative effect of the irradiation of collagen. Consequently, all parameters should be carefully investigated to clarify the alteration of fibroblasts after laser irradiation.

Conclusions

The results reported here demonstrate that successive LLRL irradiation of collagen thin films and solutions caused a small increase in the intensity of the emitted fluorescence. AFM nanocharacterization of collagen thin films demonstrated that surface topography was not altered after irradiation, and the surface roughness of the films remained almost constant. Moreover, after irradiation, the D-periodicity of collagen fibers did not show any significant modifications. The use of

LLRL-irradiated collagen thin films as a cell substrate showed that increased irradiation repetition induced abnormal growth in fibroblasts. The bodies and nuclei of fibroblasts became more spherical, and they showed larger numbers of filopodia. The results of this study show for the first time, to the best of our knowledge, the effect of LLRL irradiation on pure collagen. Although irradiation did not affect the nanotopography of collagen, cell behavior was influenced. Because altered cell behavior was observed in the absence of measurable surface alterations, it can be inferred that cell–surface interactions/guidance based on surface characteristics were not responsible for modification of cell growth. The role of collagen in the LLLT mechanism appears to be crucial, and our results demonstrate that collagen affects not only the cell function but also collagen itself.

Acknowledgments The authors are grateful to Dr. D. Kletsas from the Laboratory of "Cell Proliferation and Ageing" of the National Center for Scientific Research "Demokritos" for kindly providing the human fibroblasts primary cell line.

Compliance with ethical standards

Funding This research has been co-financed by the European Union (European Social Fund, ESF) and Greek national funds through the Operational Program "Education and Lifelong Learning" of the National Strategic Reference Framework (NSRF)—Research Funding Program: Heracleitus II. Investing in knowledge society through the European Social Fund.

References

1. Mandel A, Hamblin MR (2012) A renaissance in low-level laser (light) therapy—LLLT. Photonics and Lasers in Med 1(4):231–234. doi:10.1515/plm-2012-0044
2. Chung H, Dai T, Sharma SK, Huang YY, Carroll JD, Hamblin MR (2012) The nuts and bolts of low-level laser (light) therapy. Ann Biomed Eng 40:516–533. doi:10.1007/s10439-011-0454-7
3. Farivar S, Malekshahabi T, Shiari R (2014) Biological effects of low level laser therapy. J Lasers Med Sci 5(2):58–62
4. AlGhamdi KM, Kumar A, Moussa NA (2012) Low-level laser therapy: a useful technique for enhancing the proliferation of various cultured cells. Lasers Med Sci 27(1):237–249. doi:10.1007/s10103-011-0885-2
5. Gupta A, Dai T, Hamblin MR (2014) Effect of red and near-infrared wavelengths on low-level laser (light) therapy-induced healing of partial-thickness dermal abrasion in mice. Lasers Med Sci 29(1):257–265. doi:10.1007/s10103-013-1319-0
6. Lyons RF, Abergel RP, White RA, Dwyer RM, Castel JC, Uitto J (1987) Biostimulation of wound healing in vivo by a helium-neon laser. Ann Plast Surg 18(1):47–50. doi:10.1097/00000637-198701000-00011
7. Hawkins D, Houreld N, Abrahamse H (2005) Low level laser therapy (LLLT) as an effective therapeutic modality for delayed wound healing. Ann N Y Acad Sci 1056:486–493. doi:10.1196/annals.1352.040
8. Fiório FB, Albertini R, Leal-Junior ECP, de Carvalho PTC (2013) Effect of low-level laser therapy on types I and III collagen and inflammatory cells in rats with induced third-degree burns. Lasers Med Sci 29(1):1–7. doi:10.1007/s10103-013-1341-2
9. Pugliese LS, Medrado AP, Reis SR, Andrade ZA (2003) The influence of low-level laser therapy on biomodulation of collagen and elastic fibers. Pesqui Odontol Bras 17(4):307–313
10. Hawkins DH, Abrahamse H (2006) The role of laser fluence in cell viability, proliferation, and membrane integrity of wounded human skin fibroblasts following helium-neon laser irradiation. Lasers Surg Med 38(1):74–83. doi:10.1002/lsm.20271
11. Fushimi T, Inui S, Nakajima T, Ogasawara M, Hosokawa K, Itami S (2012) Green light emitting diodes accelerate wound healing: characterization of the effect and its molecular basis in vitro and in vivo. Wound Repair Regen 20(2):226–235. doi:10.1111/j.1524-475X.2012.00771.x
12. Peplow PV, Chung TY, Baxter GD (2012) Laser photostimulation (660nm) of wound healing in diabetic mice is not brought about by ameliorating diabetes. Lasers Surg Med 44(1):26–29. doi:10.1002/lsm.21133
13. Fratzl P (2008) Collagen structure and mechanics. Book, Edited. Springer, New York. doi: 10.1007/978-0-387-73906-9
14. Heino J (2007) The collagen family members as cell adhesion proteins. Bioessays 29(10):1001–1010. doi:10.1002/bies.20636
15. Kadler KE, Baldock C, Bella J, Boot-Handford RP (2007) Collagens at a glance. J Cell Sci 120(12):1955–1958. doi:10.1242/jcs.03453
16. Tsai SW, Cheng YH, Chang Y, Liu HL, Tsai WB (2010) Type I collagen structure modulates the behavior of osteoblast-like cells. J Taiwan Inst Chem E 41(3):247–251. doi:10.1016/j.jtice.2009.10.002
17. Plant AL, Bhadriraju K, Spurlin TA, Elliott JT (2009) Cell response to matrix mechanics: focus on collagen. Biochim Biophys Acta 1793(5):893–902. doi:10.1016/j.bbamcr.2008.10.012
18. Stylianou A, Yova D, Alexandratou E (2013) Nanotopography of collagen thin films in correlation with fibroblast response. J Nanophotonics 7(1):073590. doi:10.1117/1.JNP.7.073590
19. Medrado AP, Soares AP, Santos ET, Reis SRA, Andrade ZA (2008) Influence of laser photobiomodulation upon connective tissue remodeling during wound healing. J Photochem Photobiol B 92(3):144–152. doi:10.1016/j.jphotobiol.2008.05.008
20. Garavello-Freitas I, Baranauskas V, Joazeiro PP, Padovani CR, Dal Pai-Silva M, da Cruz-Höfling MA (2003) Low-power laser irradiation improves histomorphometrical parameters and bone matrix organization during tibia wound healing in rats. J Photochem Photobiol B 70(2):81–89. doi:10.1016/s1011-1344(03)00058-7
21. Fung DTC, Ng GYF, Leung MCP, Tay DKC (2003) Effects of a therapeutic laser on the ultrastructural morphology of repairing medial collateral ligament in a rat model. Lasers Surg Med 32(4):286–293. doi:10.1002/lsm.10161
22. Stylianou A, Kontomaris SB, Kyriazi M, Yova D (2010) Surface characterization of collagen films by atomic force microscopy. In: 12th Mediterranean Conference on Medical and Biological Engineering and Computing, MEDICON 2010. pp 612–615. doi:10.1007/978-3-642-13039-7_154
23. Stylianou A, Yova D, Politopoulos K (2012) Atomic force microscopy quantitative and qualitative nanoscale characterization of collagen thin films. In: 5th International Conference on Emerging Technologies in Non-Destructive Testing. NDT 2012:415–420. doi:10.1201/b11837-75
24. Baranauskas V, Garavello I, Jingguo Z, Da Cruz-Höfling MA (2005) Analyses of regenerative bone matrix of rat tibia after laser photo-excitation by SEM and AFM. Appl Surf Sci 248(1–4):492–498. doi:10.1016/j.apsusc.2005.03.097

25. Stylianou A, Yova D (2013) Surface nanoscale imaging of collagen thin films by atomic force microscopy. Mater Sci Eng C Mater Biol Appl 33(5):2947–2957. doi:10.1016/j.msec.2013.03.029
26. Stylianou A, Politopoulos K, Kyriazi M, Yova D (2011) Combined information from AFM imaging and SHG signal analysis of collagen thin films. Biomed Signal Proces 6(3):307–313. doi:10.1016/j.bspc.2011.02.006
27. França CM, Núñez SC, Prates RA, Noborikawa E, Faria MR, Ribeiro MS (2009) Low-intensity red laser on the prevention and treatment of induced-oral mucositis in hamsters. J Photochem Photobiol B 94(1):25–31. doi:10.1016/j.jphotobiol.2008.09.006
28. Lakowicz J (1999) Principles of fluorescence spectroscopy. Kluwer Academic/Plenum Publishers, New York
29. Alexandratou E, Yova D, Handris P, Kletsas D, Loukas S (2002) Human fibroblast alterations induced by low power laser irradiation at the single cell level using confocal microscopy. Photochem Photobiol Sci 1(8):547–552. doi:10.1039/b110213n
30. Horcas I, Fernández R, Gómez-Rodríguez JM, Colchero J, Gómez-Herrero J, Baro AM (2007) WSXM: A software for scanning probe microscopy and a tool for nanotechnology. Rev Sci Instrum 78(1). doi:10.1063/1.2432410
31. Wu K, Liu W, Li G (2013) The aggregation behavior of native collagen in dilute solution studied by intrinsic fluorescence and external probing. Spectrochim Acta A Mol Biomol Spectrosc 102:186–193. doi:10.1016/j.saa.2012.10.048
32. Torikai A, Shibata H (1999) Effect of ultraviolet radiation on photodegradation of collagen. J Appl Polym Sci 73(7):1259–1265
33. Silver FH, Freeman JW, Seehra GP (2003) Collagen self-assembly and the development of tendon mechanical properties. J Biomech 36(10):1529–1553. doi:10.1016/s0021-9290(03)00135-0
34. Tunér J, Hode L (1998) It's all in the parameters: a critical analysis of some well-known negative studies on low-level laser therapy. J Clin Laser Med Surg 16(5):245–248
35. Odetti PR, Borgoglio A, Rolandi R (1992) Age-related increase of collagen fluorescence in human subcutaneous tissue. Metabolism 41(6):655–658. doi:10.1016/0026-0495(92)90059-j
36. Sell DR, Nemet I, Monnier VM (2010) Partial characterization of the molecular nature of collagen-linked fluorescence: role of diabetes and end-stage renal disease. Arch Biochem Biophys 493(2):192–206. doi:10.1016/j.abb.2009.10.013
37. Perez Gutierrez RM (2012) Inhibition of advanced glycation end-product formation by Origanum majorana L. in vitro and in streptozotocin-induced diabetic rats. Evid Based Complement Alternat Med 2012, art. no. 598638. doi: 10.1155/2012/598638
38. Dina RC, Vladu I, Dina CA, Mitrea A (2012) Advanced glycation end products measured by AGE Reader in a group of patients with obesity. Rom J Diabetes Nutr Metab Dis 19(1):59–66
39. Babu PVA, Sabitha KE, Shyamaladevi CS (2008) Effect of green tea extract on advanced glycation and cross-linking of tail tendon collagen in streptozotocin induced diabetic rats. Food Chem Toxicol 46(1):280–285. doi:10.1016/j.fct.2007.08.005
40. Stylianou A, Yova D, Alexandratou E, Petri A (2013) Atomic force imaging microscopy investigation of the interaction of ultraviolet radiation with collagen thin films. In: Nanoscale Imaging, Sensing, and Actuation for Biomedical Applications X, 2013 2012. doi:10.1117/12.2002460
41. Loesberg WA, te Riet J, van Delft FCMJM, Schön P, Figdor CG, Speller S, van Loon JJWA, Walboomers XF, Jansen JA (2007) The threshold at which substrate nanogroove dimensions may influence fibroblast alignment and adhesion. Biomaterials 28(27):3944–3951. doi:10.1016/j.biomaterials.2007.05.030
42. Engler AJ, Sen S, Sweeney HL, Discher DE (2006) Matrix elasticity directs stem cell lineage specification. Cell 126(4):677–689. doi:10.1016/j.cell.2006.06.044
43. Spurlin TA, Bhadriraju K, Chung KH, Tona A, Plant AL (2009) The treatment of collagen fibrils by tissue transglutaminase to promote vascular smooth muscle cell contractile signaling. Biomaterials 30(29):5486–5496. doi:10.1016/j.biomaterials.2009.07.014
44. Fassett J, Tobolt D, Hansen LK (2006) Type I collagen structure regulates cell morphology and EGF signaling in primary rat hepatocytes through cAMP-dependent protein kinase A. Mol Biol Cell 17(1):345–356. doi:10.1091/mbc.E05-09-0871
45. Ross AM, Jiang Z, Bastmeyer M, Lahann J (2012) Physical aspects of cell culture substrates: topography, roughness, and elasticity. Small 8(3):336–355. doi:10.1002/smll.201100934